ELSEVIER

Desalination 179 (2005) 281–295

DESALINATION

www.elsevier.com/locate/desal

Inorganic foulants in membrane systems: chemical control strategies and the contribution of "green chemistry"

Konstantinos D. Demadis*, Eleftheria Neofotistou, Eleftheria Mavredaki, Michalis Tsiknakis, Eva-Maria Sarigiannidou, Stella D. Katarachia

Department of Chemistry, University of Crete, Heraklion GR-71409 Crete, Greece
Tel. +30 (2810) 393651, Fax: +30 2810 393601; email: demadis@chemistry.uoc.gr;
http://www.chemistry.uco.gr/en/personnel/faculty/demadis.htm

Received 16 September 2004; accepted 22 November 2004

Abstract

Colloidal silica (SiO_2) and other sparingly soluble salts such as $CaCO_3$ present a challenge for desalination systems used for brackish or seawater desalting. When SiO_2 is left uncontrolled, it forms hard and tenacious deposits that are difficult and hazardous to remove. Conventional phosphonate mineral scale inhibitors do not inhibit SiO_2 formation and deposition. Chemical cleaning is not free from hazards and requires operational shut-downs. $CaCO_3$ is also troublesome. This paper focused on silica and $CaCO_3$ formation, deposition and inhibition with designed chemical approaches in water applications that require the use of membranes. It also describes SiO_2 scale removal by dissolution approaches with environmentally friendly and non-hazardous chemical additives. The general scope of silica formation and inhibition in waters relevant to desalination systems is also discussed. This paper continues our research efforts in the discovery, design and application of anti-scalant additives that have a mild environmental impact. These chemicals are also known as "green additives". In light of increasing environmental concerns for discharge of saline water coming from desalination systems, this research is of significant interest.

Keywords: Membrane fouling; Scale; Inhibition; Dissolution; Cleaning; Green additives; Silica; Calcium carbonate

1. Introduction

Membrane systems in brackish or seawater desalination operations are often plagued by deposition problems that originate from a variety of deposits, organic or inorganic [1]. The latter, often known as mineral scale deposits, can become major operational issues for poorly treated process waters [2]. Some of these, such as silica, are especially troublesome because they can cause catastrophic operational failures in sea or

*Corresponding author.

Presented at the conference on Membranes in Drinking and Industrial Water Production, L'Aquila, Italy, 15–17 November 2004. Organized by the European Desalination Society.

0011-9164/05/$– See front matter

Fig. 1. Silica scale deposits on a RO membrane surface.

brackish water desalination systems (Fig. 1) [3,4]. Industrial and potable water users and operators are often faced with a challenging dilemma: is it preferable to prevent deposits from forming, or is it better to clean the deposits after they form? Cost considerations are usually the decision criteria, although other factors are taken into account as well (e.g., potential hazards of cleaning chemicals) [5].

Scale prevention in principle can be achieved by use of scale inhibitors, key components of any chemical water treatment [6]. Unfortunately, these traditional scale control methods (inhibition and crystal modification) applied to crystalline mineral salt precipitates *do not apply to* SiO_2 *because it is amorphous*. Therefore, much more well-thought inhibition approaches have to be utilized for controlling silica scale.

Increasing environmental concerns and discharge limitations have imposed additional challenges in treating process waters. Therefore, the discovery and successful application of chemical additives that have a mild environmental impact have been the focus of several researchers [7]. This paper focuses on use of "green" inhibitors in synergistic action with "green" polymers for (a) silica/silicate scale inhibition, (b) $CaCO_3$ scale inhibition and (c) silica scale dissolution. This research is part of our on-going investigation on the discovery and application of scale inhibitors in industrial process waters [8–12].

2. Experimental

Detailed procedures for some of the instruments used, reagents, solution preparation, inhibitor screening test, soluble silica measurement are reported elsewhere [13].

2.1. Scale monitoring instrumentation

A Model 55T photo-X transmitter was provided by Custom Sensors & Technology (St. Louis, MO, USA). It is configured as a continuous photometric transmitter coupled with a scale sensor that provides for analysis of a process liquid stream. The span of concentration covered is selected by a combination of path length and transmitter control settings. Scale deposits on the scale sensor cause an increase in absorbance and are indicative of surface fouling.

2.2. Reagents

Model silica for the dissolution studies was Aerosil 200 from Degussa, carboxymethylinulin (CMI) from Solutia, citric acid from Riedel de Haen, oxalic acid dihydrate from E.M. Science Merck, 2-phosphonobutane-1,2,4-tricarboxylic acid (commercial name Dequest 7000, 50% w/w active acid) from Solutia, diethylenetriaminepentacetic acid from Aldrich, and ammonium bifluride (in the form of crystalline $NH_4HF{\cdot}HF$) from Fischer.

2.3. Silica inhibition protocol

Details can be found elsewhere [13].

2.4. Silica dissolution protocol

Glass containers must be avoided in order to

minimize silica leach out. A quantity of solid SiO_2 (Aerosil 200) corresponding to 500 ppm as SiO_2 (calculated for 100 mL final solution volume) was placed in a polyethylene container with 80 mL deionized water and a dosage of specific chemical additive (1,000–11,000 ppm). In some cases chemical additives do not dissolve readily; therefore, addition of a small amount of NaOH or mild heating may be necessary to achieve complete dissolution of the additives. Then, solution pH is adjusted to 10.00 by use of NaOH or HCl (10%). Finally, solutions were diluted up to 100 mL and kept under continuous stirring for the next 72 h. Soluble silica measurements on small samples withdrawn were made at 24, 48 and 72 h. After each measurement pH was again checked, and in case of deviation from the target value, a readjustment was made.

2.5. Interference test

Every cleaning additive was tested for its interference with the silicomolybdate spectrophotometric test. A stock solution (500 ppm) of soluble SiO_2 (from sodium silicate) was prepared. To 100 mL of that solution a dosage of the cleaning chemical was added. After appropriate dilutions were made, soluble silica was measured and the results compared to the expected value of 500 ppm. Additives that interfere with the test were rejected.

2.6. $CaCO_3$ formation and inhibition monitoring test

The protocol involving AMP and the dispersant polymer can be found elsewhere [11,12]. $CaCO_3$ growth experiments using the scale sensor were performed following the following procedure. Stock solutions of $CaCl_2{\cdot}2H_2O$ and $NaHCO_3$ (both 5×10^{-2} M) were prepared. Volumes of 80 mL $CaCl_2{\cdot}2H_2O$ and 80 mL $NaHCO_3$ stock solutions were mixed under continuous stirring and the pH was adjusted to 7.5 with dilute NaOH. For the inhibition experiments the above procedure was followed, except that the appropriate amount of inhibitor solution was added to reach the desired active inhibitor dosage. The absorbance on the scale sensor display was monitored at appropriate time intervals and recorded. The experiment was stopped when there was no increase in absorbance values.

3. Results

High dissolved silica content in process waters used for industrial applications leads to formation of colloidal silica that is deposited onto critical surfaces and forms a hard and tenacious deposit that is not easily removed [14]. Silica scale may require unconventional means to be controlled. Other, more traditional approaches, still utilize chemicals for water treatment in order to prevent silica scale formation and deposition. Silica and/or silicate deposits are particularly difficult to remove and usually require harsh chemical cleaning (with hydrofluoric acid) or mechanical removal [15–17].

3.1. "Green" scale inhibitors

Herein we report results on the inhibition performance of several environmentally friendly anti-scalants. Some comments are warranted. Polyaminoamide dendrimers (PAMAMs) have been used for medical applications (e.g., as drug delivery agents) [18]; therefore, they are undoubtedly benign and non-toxic molecules. A representative schematic structure of PAMAM (Generation 1) is shown in Fig. 2.

Polyethyloxazoline polymers of various molecular weights are additives approved by the FDA for use as an indirect food additive (adhesive) under 21 CFR 175.105 [19]. The oral toxicity was measured LD50 (rat): 3980 mg/kg. These polymers were also not found to be in any hazard category defined by SARA Title III, Sections 311 and 312. Their structure is shown in Fig. 3.

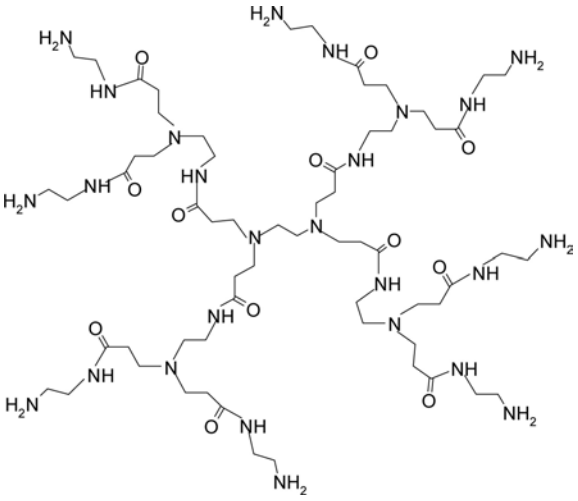

Fig. 2. Schematic structure of PAMAM (Generation 1), with 8 $-NH_2$ terminal moieties.

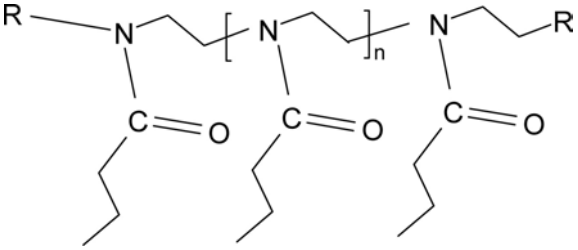

Fig. 3. Schematic structure of polyethyloxazoline (AQUAZOL) polymers.

Carboxymethylinulin (CMI) [20] (Fig. 4) is produced from a chemical reaction of a biopolymer and select reagents. This biopolymer, inulin, is extracted from the roots of the chicory plant. The leaves of this plant are used in salads in the US and Europe while the roots are used in the southern US to flavor coffee and even substitute for coffee. The biopolymer inulin backbone is a polysaccharide composed of d-fructose units linked at the 1 and 2 position and end-capped with a d-glucose.

CMI has been investigated in a series of subacute toxicity, genotoxicity and sensitization studies to evaluate its toxicological profile [20]. All studies followed accepted testing guidelines

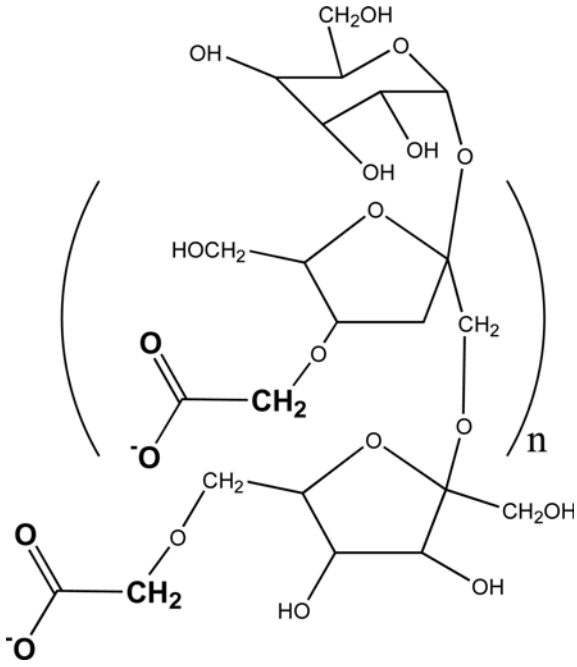

Fig. 4. Schematic structure of carboxymethylinulin biopolymer. The "active" carboxylate groups are highlighted in bold.

as recommended by international regulatory agencies (OECD, EEC and US EPA). No significant toxicological findings were evident. No evidence of genotoxicity was observed in studies *in vitro* designed to identify agents capable of producing point mutations or chromosomal aberrations. CMI did not induce a dermal sensitization response in guinea pigs, nor did it produce irritation following extended epidermal application. With few exceptions, no consistent pattern of altered toxicological endpoints was identified in a repeated dose toxicity study in rats. Results of the present toxicity studies with CMI, all conforming to internationally accepted testing standards, show that the toxicological profile of CMI is consistent with other polycarboxylates used in foods.

AMP (Fig. 5) is a chelating agent that is commonly used to retard the precipitation/crystallization of sparingly soluble salts from process

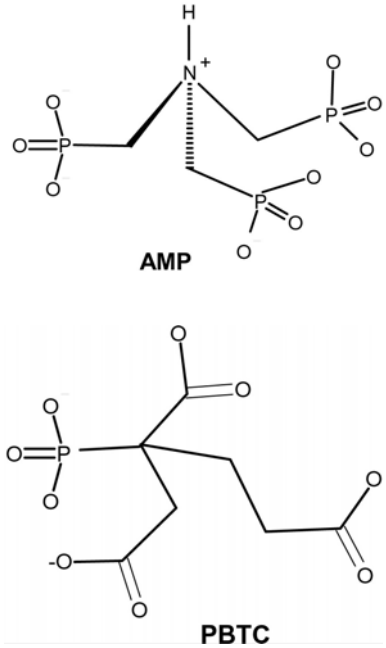

Fig. 5. Chemical structures of amino-*tris*-(methylene-phosphonate) (AMP), and 2-phosphonobutane-1,2,4-tricarboxylic acid (PBTC) in their fully deprotonated forms.

waters [21]. Published work on the environmental behavior of AMP reported that from results of several discontinuous and semi-continuous model tests, no evidence for biodegradability of AMP could be obtained [22]. More recent studies showed that AMP is transformed both in aerobically incubated natural and synthetic aqueous media and soils to degradation products. In the presence of microorganisms, AMP is slowly degraded to aminomethylene-monophosphonate. It was also concluded that AMP does not undergo significant degradation within the retention times of wastewaters in sewage plants [23,24]. However, in surface waters a fast and quantitative abiotic degradation is expected yielding the biodegradable aminomethylene-monophosphonate.

PBTC [25] (Fig. 5) is a very robust molecule and is studied herein in silica dissolution studies for comparison to citrate, a tricarboxylate that possesses certain similarities with PBTC.

3.2. Dendrimers as silica anti-scalants

We recently reported in detail the use of dendrimers for silica scale control [9,10,13]. Those findings revealed that the -COOH terminated dendrimers show virtually no activity as inhibitors. In contrast, the -NH_2 terminated analogs are potent silica scale inhibitors.

In spite of the excellent performance of PAMAM 1 and 2 dendrimers as "green" colloidal silica inhibitors, they suffer from a serious drawback: the silicate levels that are not inhibited lead to the formation of large colloidal silica particles that entrap the dendrimers. Visual observations show that these particles appear as white flocculant precipitates at the bottom of the test vessels. Chemical analysis by X-ray diffraction of these amorphous precipitates showed that they are principally composed of silica (>90%), with the rest being organic material, undoubtedly dendrimer. FT-IR spectroscopy also verified the presence of silica (several characteristic bands) [13], but also the presence of the PAMAM dendrimers (the amide ν(C=O) appears at 1645 cm^{-1}).

Formation of SiO_2-PAMAM precipitates occurs due to the combination of anionic SiO_2 particles and cationic PAMAM-1 or 2 dendrimers. To combat this problem, we resorted to utilization of anionic polymer additives. Herein, we describe the effect of CMI on the performance of the PAMAM dendrimers. Table 1 and Fig. 6 show the results obtained from experiments performed where the PAMAM-1 dendrimer and CMI were both present in solution. Table 2 and Fig. 7 show analogous results obtained with the PAMAM-2 dendrimer and CMI. It should be noted that dendrimets with -COOH terminal groups (generations 0.5, 1.5 and 2.5) were not tested because their inhibition performance is indistinguishable from the control. When PAMAM 1 is used at 40 ppm levels together with 20 ppm CMI, 408 ppm of soluble SiO_2 are measured within 24 h. This level drops at 381 ppm

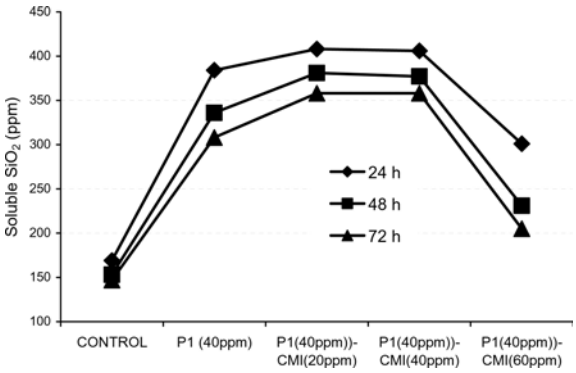

Fig. 6. Effect of PAMAM-1 dendrimer and CMI combinations on soluble SiO_2.

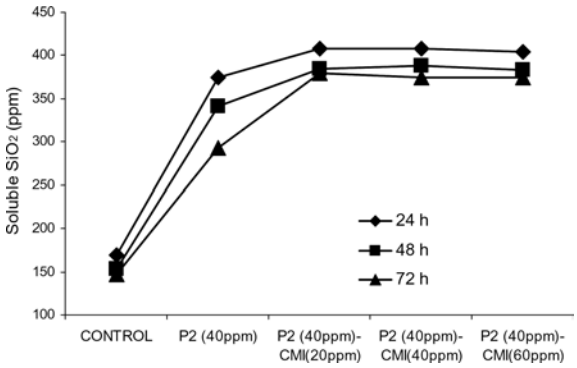

Fig. 7. Effect of PAMAM-2 dendrimer and CMI combinations on soluble SiO_2.

Table 1
Effect of CMI (dosage 20, 40 and 60 ppm) on SiO_2 inhibition performance of PAMAM-1 dendrimer (40 ppm)

		Soluble SiO_2 (ppm)			
Time (h)	Control	PAMAM-1 (40 ppm) no CMI added	PAMAM-1 (40 ppm) CMI (20 ppm)	PAMAM-1 (40 ppm) CMI (40 ppm)	PAMAM-1 (40 ppm) CMI (60 ppm)
24	169	384	408	406	301
48	153	336	381	377	231
72	147	308	358	358	205

Table 2
Effect of CMI (dosage 20, 40 and 60 ppm) on SiO_2 inhibition performance of PAMAM-2 dendrimer (40 ppm)

		Soluble SiO_2 (ppm)			
Time (h)	Control	PAMAM-1 (40 ppm) no CMI added	PAMAM-1 (40 ppm) CMI (20 ppm)	PAMAM-1 (40 ppm) CMI (40 ppm)	PAMAM-1 (40 ppm) CMI (60 ppm)
24	169	374	408	408	404
48	153	341	385	388	383
72	147	293	380	375	375

and 308 ppm after 48 and 72 h, respectively. In general, a drop in soluble silica levels occurs also in control solutions (see Table 1), regardless of the presence of inhibitor. Increase of CMI dosage to 40 ppm seems to have no effect on soluble silica. However, an increase of the CMI dosage to 60 ppm has a detrimental effect on maintaining high levels of soluble silica. A level of 301 ppm soluble silica (a drop of ~100 ppm) was observed after of 24 h, compared to 408 ppm when 20 ppm of CMI are present.

A similar trend was observed in solutions

containing both PAMAM-2 and CMI. When PAMAM-2 is used with CMI, 408 ppm soluble SiO_2 were measured after 24 h, 385 ppm after 48 h and 380 ppm after 72 h. It is worth mentioning that soluble SiO_2 levels are higher in solutions containing PAMAM-2 + CMI than those containing PAMAM-1 + CMI.

An increase of the CMI dosage to 40 ppm gives results virtually indistinguishable from those obtained with 20 ppm CMI. Interestingly, a further increase of CMI dosage to 60 ppm does not cause a drop in soluble silica levels, as observed with 40 ppm PAMAM-1 and 60 ppm CMI.

The above observations can be interpreted upon examination of the nature of the CMI biopolymer. CMI is an anionic polyelectrolyte possessing -COOH groups that readily associate in solution in the presence of cationic PAMAM-1 or 2. Thus, its deprotonated -COO^- groups partially "neutralize" the positive charge on the dendrimer peripheral groups (-NH_3^+). This in turn alleviates SiO_2–PAMAM precipitate formation, perhaps by "protecting" the dendrimer from being incorporated into the colloidal silica matrix, resulting into deactivation. When the anionic CMI biopolymer is added in excess (60 ppm), the negative charge on the polymer backbone exceeds the positive charge on the dendrimer molecule, resulting in a drop of activity. It should be noted that the presence of positively charged groups alone is not the only structural property necessary for inhibitory activity. Studies (not shown here) with NH_4^+ or $(CH_3CH_2)_4N^+$ as potential inhibitors show that these "small" molecules are completely inactive in preventing SiO_2 polymerization. The positive charge sites in the structures of PAMAM-1 or 2 dendrimers are positioned in such a way that they effectively "interfere" with SiO_2 polymerization resulting in inhibition. Therefore, the overall structure certainly plays a profound role. The effect of CMI addition is obvious. There is no precipitate formed except a slight dispersion that does not settle, but persists for several months.

3.3. Poly(2-ethyl-2-oxazoline) (Aquazol) polymers as silica antiscalants

The experiments carried out with the PAMAM dendrimers as inhibitors prompted us to consider other macromolecules that possess similar structural features to the dendrimers (e.g., amide bonds), but are more cost effective. We resorted to polymers called poly(2-ethyl-2-oxazolines) (commercial name, Aquazols).

Aquazol polymers are available in molecular weights of 5,000, 50,000, 200,000 and 500,000. The same inhibition test was followed as that used for the dendrimers. We chose to present results with two Aquazol polymers, 50 and 500. In Table 3 and Fig. 8 inhibition results are presented using Aquazol-50 at 20, 40, 60 and 80 ppm dosages. It should be noted that virtually all Aquazol polymers show good inhibition results, with Aquazol 5 being the least effective. It appears that all the other Aquazol polymers exhibit very similar inhibition properties that are independent of their molecular weight (results not shown here). Table 4 and Fig. 9 show inhibition results using Aquazol-500 at 20, 40, 60 and 80 ppm dosages.

The dependence of SiO_2 inhibition on Aquazol polymer dosage reveals that the dose–response relationship is "normal". This means that as the inhibitor dosage increases, inhibition efficiency improves as well. This appears to be in contrast to the dendrimer inhibition behavior [13]. When PAMAM-1 and -2 are the only scale-inhibiting molecules in solution, they show a maximum effectiveness at 40 ppm dosage, but a further increase (60 or 80 ppm) results into dramatic loss of inhibitory activity.

Aquazols, when used at 20 ppm dosage, exhibit low inhibition efficiency, barely higher than the control. At 40 ppm dosage both polymers improve in retarding SiO_2 growth after 24 h. This tendency is more evident when 60 ppm inhibitors are present. There appears to be a "jump" in inhibitor performance at this level. At 80 ppm

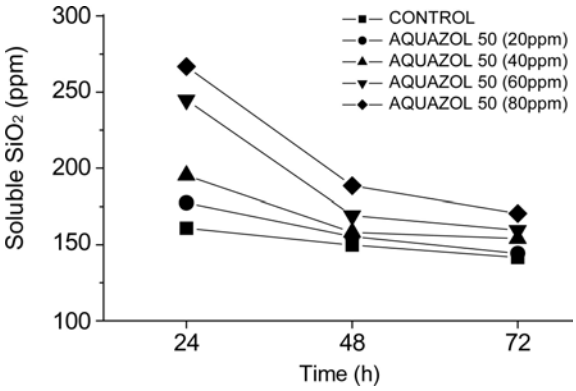

Fig. 8. Effect of various dosages of Aquazol-50 polymer on SiO_2 polymerization.

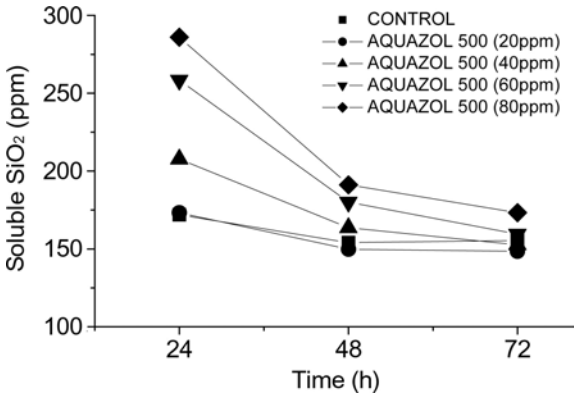

Fig. 9. Effect of various dosages of Aquazol-500 polymer on SiO_2 polymerization.

Table 3
Effect of Aquazol-50 polymers on SiO_2 polymerization

		Soluble SiO_2 (ppm)			
Time (h)	Control	Aquazol 50 (20 ppm)	Aquazol 50 (40 ppm)	Aquazol 50 (60 ppm)	Aquazol 50 (80 ppm)
24	161	177	195	245	267
48	150	155	158	169	188
72	142	144	154	160	171

Table 4
Effect of Aquazol-500 polymer on SiO_2 polymerization

		Soluble SiO_2 (ppm)			
Time (h)	Control	Aquazol 50 (20 ppm)	Aquazol 50 (40 ppm)	Aquazol 50 (60 ppm)	Aquazol 50 (80 ppm)
24	161	173	208	259	286
48	150	150	164	180	191
72	142	149	153	160	173

inhibitor level there is even better SiO_2 inhibition. Both Aquazol-50 and 500 show a markedly decreased efficiency after 48 h but maintain SiO_2 soluble at levels higher than the control. It should be noted that after 72 h the soluble SiO_2 levels were essentially similar to those measured at 48 h. This means that the inhibitor efficiency, albeit somewhat reduced, is still maintained.

3.4. Magnesium silicate scale inhibition

Magnesium silicate is one of the poorly studied foulants [26–28]. It is not widespread in water systems, but rather limited to those waters that satisfy three conditions: (a) contain high levels of silica, (b) contain high levels of magnesium, and (c) operate at high pH regions

(>8.5). This is mentioned here because it relates to silica.

Ca^{2+} and Mg^{2+} salts were found to catalyze the silica polymerization reaction [29]. Higher concentrations of total hardness lead to a faster drop in dissolved silica in solution. In batch runs, Mg^{2+} was found to affect silica concentrations more than Ca^{2+}. Runs with a given hardness level but with lower ratios of Ca:Mg caused faster decline in dissolved silica.

Magnesium silicate exhibits "inverse solubility" properties [30,31]. This means that its precipitation is more pronounced as the temperature of bulk water increases. Similar behavior is shown by a plethora of other sparingly soluble salts, such as $CaCO_3$, $CaSO_4$, etc.

Precipitation and deposition of magnesium silicate is largely driven by pH. This is clearly shown in Fig. 10 by the dramatic increase in Mg content in the deposited scale as the pH is increased. Additional details on magnesium silicate precipitation and inhibition will be given in a future publication.

3.5. Dissolution of colloidal silica

The solubility of SiO_2 increases as pH increases [32,33]. Therefore, high pH regions are desirable for SiO_2 scale dissolution. However, SiO_2 chemical cleanings have to be performed at pH regions that do not compromise system integrity and personnel safety. In the experiments reported herein, a pH of 10.00 was selected. Various "green" additives were tested. A dicarboxylate (oxalic acid), a tricarboxylate (citric acid), a mixed monophosphonate/tricarboxylate (2-phosphonobutane-1,2,4-tricarboxylic acid), a pentacarboxylate (diethylenetriaminepentaacetic acid), and a polycarboxylate biopolymer (CMI) were tested as silica scale dissolvers. Ammonium bifluoride, $NH_4F{\cdot}HF$, was also included in the study because it is currently used for cleaning SiO_2/silicate deposits in industrial water systems. Hazards associated with generating HF *in situ*, as well as the low pH of the dissolution process and the resulting high metallic corrosion rates during cleaning, are some of the reasons that alternative, safer and more effective chemical approaches are sought for SiO_2/silicate deposit dissolution.

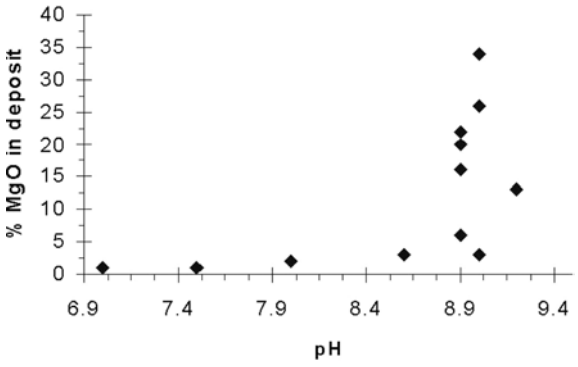

Fig. 10. Effect of pH on magnesium silicate deposition.

Results are presented in Table 5 and shown in Figs. 11–14. SiO_2 dissolution in the absence of additives proceeds fairly slowly with time, reaching ~200 ppm soluble SiO_2. There exists some variability in results that is most likely due to small differences in solution stirring rates. In the case of oxalic, citric, and diethylenetriaminepentaacetic acid, SiO_2 dissolution appears to be independent of additive dosage throughout the experiment. Citric and oxalic acids accelerate SiO_2 dissolution, eventually dissolving ~200 ppm and 230 ppm, respectively (after 72 h). Diethylenetriaminepentaacetic acid is a more effective dissolver allowing 270 ppm of SiO_2 to dissolve. 2-phosphonobutane-1,2,4-tricarboxylic acid is the most effective cleaner. When used at 11,000 ppm dosage, it dissolves 333 ppm SiO_2, a 67% dissolution efficiency.

Independent experiments were performed with all the aforementioned additives at pH 9.00. As expected, soluble SiO_2 levels were lower than those at pH 10.00 (results not shown).

Ammonium bifluoride, although added in fairly low dosages, is an effective cleaner. It should be noted that it is a superior dissolver at pH 4 than at pH 6.

Table 5
SiO_2 dissolution in the presence of various additives

Chemical additive	pH	Dosage (ppm)	Soluble SiO_2 (ppm)		
			24 hours	48 hours	72 hours
Citric acid	10	0	78	153	191
		4000	129	193	208
		8000	140	191	208
		10000	139	194	224
Oxalic acid	10	0	128	153	164
		2000	133	172	204
		4000	122	184	182
		8000	139	162	227
		10000	129	180	224
Diethylenetriaminepentaacetic acid	10	0	140	149	201
		4000	198	271	259
		8000	198	278	263
		10000	221	249	270
2-phosphonobutane-1,2,4-tricarboxylic acid	10	0	128	199	193
		8000	224	296	308
		10000	282	304	319
		11000	254	318	333
Ammonium bifluoride	4	0	8[a]	43[b]	—
		1000	306[a]	265[b]	—
	6	0	33[a]	53[b]	—
		1000	195[a]	175[b]	—
CMI	10	0	184	163	173
		2500	120	183	264
		5000	115	158	206
		7500	144	159	205
		10000	140	186	200

[a]Measurements taken at 18 h.
[b]Measurements taken at 42 h.

Dissolution of silica scale deposits is a challenging task in membrane systems. Cleaning chemicals have to be effective, but should not harm the structural integrity of the membrane. In addition, disposal of the cleaning chemicals is a concern since they are usually used in fairly high concentrations. Thus, use of "green" silica cleaners is a safer scale removal method.

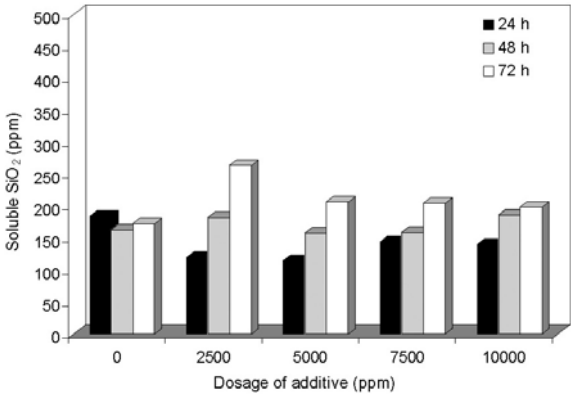

Fig. 11. SiO_2 dissolution by CMI.

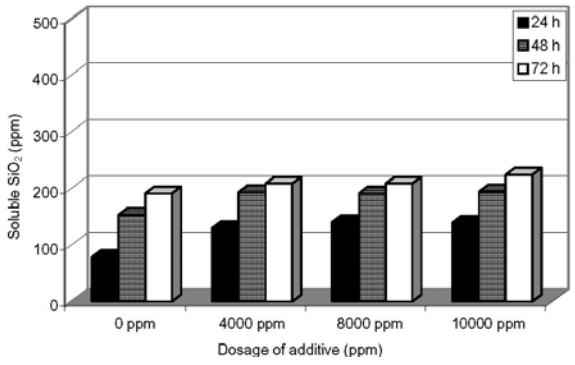

Fig. 12. SiO_2 dissolution by citric acid.

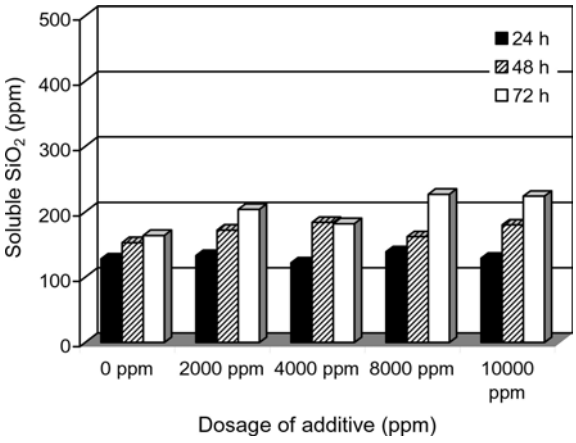

Fig. 13. SiO_2 dissolution by oxalic acid.

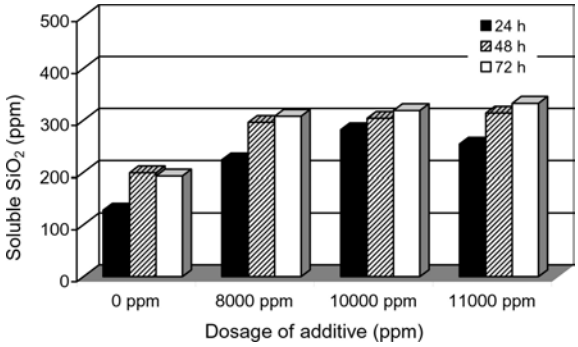

Fig. 14. SiO_2 dissolution by PBTC.

3.6. $CaCO_3$ formation and inhibition by an AMP/polymer synergistic combination

The protocol on $CaCO_3$ inhibition by AMP and the dispersant polymer can be found elsewhere [11,12]. The dispersant polymer is a proprietary chemical [34]. The efficiency of AMP as a $CaCO_3$ inhibitor was investigated at high Ca^{2+} and CO_3^{2-} levels, as well as high temperatures and pH (Table 6). $CaCO_3$ has an increased tendency to precipitate at higher temperatures, a phenomenon known as "inverse solubility". The experiments were run at 43°C. Bulk water temperatures in the range of 40–50°C are commonly found in industrial applications.

According to the results in Table 7, AMP is an effective $CaCO_3$ scale inhibitor. It can maintain 400 ppm (of 800 ppm) of soluble calcium in solution at high supersaturation and temperature (Experiment 2). Furthermore, its inhibition performance is assisted by the dispersant polymer. At lower supersaturations (Ca^{2+}/HCO_3^- of 700/700), the AMP/polymer blend achieves 75% inhibition (run 3). At higher supersaturations, however (Ca^{2+}/HCO_3^- of 900/900), the performance of the AMP/polymer blend is ~60%.

The dispersant properties of the AMP/polymer blend are measured based on dispersed Ca^{2+} (Table 7). The blend achieves quantitative dispersion of $CaCO_3$ at Ca^{2+}/HCO_3^- levels of 700/700 (Experiment 3). At higher stress conditions (Ca^{2+}/HCO_3^- of 800/800) the dispersion performance is still high at ~90% (Experiment 4), but drops to ~80% at Ca^{2+}/HCO_3^- of 900/900 (Experiment 5).

Table 6
Scale inhibition test conditions

Experiment	Ca^{2+} (ppm)	HCO_3^- (ppm)	AMP (ppm)	Polymer (ppm)
1	800	800	0	0
2	800	800	30	0
3	700	700	30	30
4	800	800	30	30
5	900	900	30	30

Table 7
Scale inhibition test results

Experiment	Soluble Ca (ppm), 2 h	% Inhibition, 2 h	Dispersed Ca (ppm), 24 h	% Dispersion, 24 h
1	5	<1	0	0
2	409	51	354	44
3	522	75	692	99
4	510	64	716	90
5	557	62	734	82

An additional point of interest is the way the AMP/polymer blend affects crystal and particle morphology of the resulting $CaCO_3$ scales. In order to examine that more carefully, samples of the $CaCO_3$ deposits were analyzed by SEM. The images are given in Fig. 15.

Upon examination of the morphology of untreated and treated $CaCO_3$ scale deposits, it becomes evident that there are obvious differences. $CaCO_3$ solids that precipitate from solutions containing no inhibiting additive are indicative of prismatic calcite (Fig. 15, upper). $CaCO_3$ solids that precipitate in the presence of the AMP/polymer blend appear as amorphous (non-crystalline) spheres and have little tendency to "stick" to each other. Their approximate size is 6 μ (Fig. 15, lower).

Dubin performed similar studies on $CaCO_3$ crystallization in the presence of organic phosphorous compounds or polymers [35]. His results showed that structural variations in organophosphonate or dispersant polymer additives used in supersaturated solutions of $CaCO_3$ caused dramatic effects on the crystal/particle morphology and size of the precipitated deposits.

3.7. $CaCO_3$ formation and dissolution by CMI

CMI was tested as a $CaCO_3$ inhibitor. Its inhibition efficiency was monitored by the scale sensor (see Experimental Section). The protocol that was followed was different from that used for the AMP/polymer synergistic study. Results are shown in Fig. 16. CMI addition in supersaturated $CaCO_3$ solutions prolongs the induction time of $CaCO_3$ formation. This is dosage dependent, as 300 ppm of CMI delay the precipitation of $CaCO_3$ by ~50 min, compared to ~20 min of the 100 ppm dosage.

After a typical $CaCO_3$ was completed there was $CaCO_3$ deposit that covered the scale sensor. A scale removal attempt was made by removing the scale probe and immersing it into a fresh solution that contained water. Then an amount of CMI was added corresponding to 10,000 ppm. Absorbance changes were again

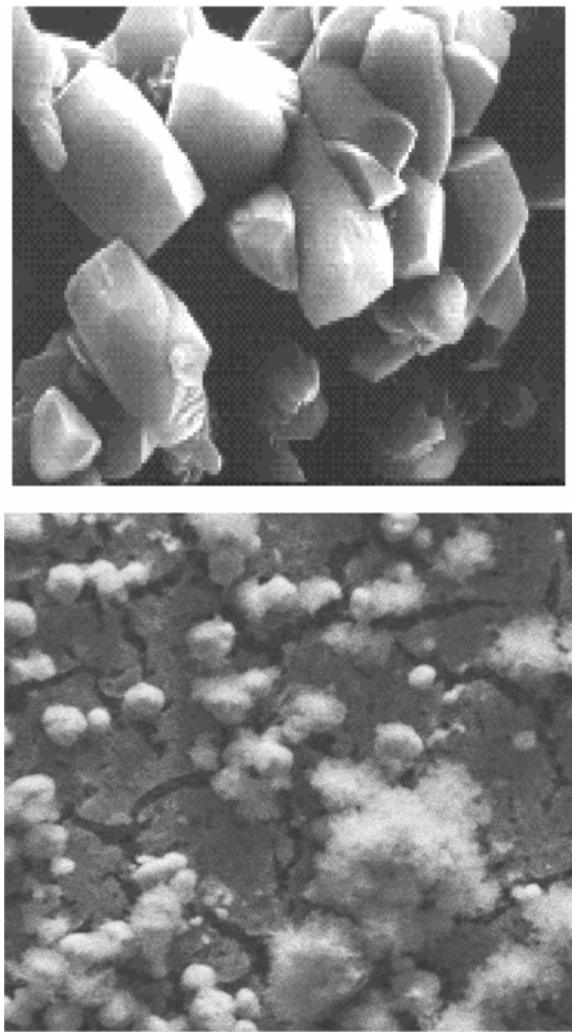

Fig. 15. Effect on the $CaCO_3$ crystal morphology of a synergistic combination of AMP/anionic polymer: no additives (upper), with 40 ppm AMP and 40 ppm polymer (lower). The width of the images corresponds to ~100 microns. The synergistic inhibitory effect of AMP and the dispersant polymer is evident in crystal size reduction and morphology changes.

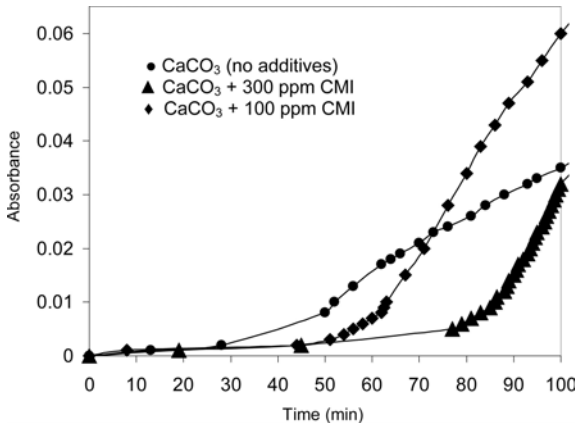

Fig. 16. Effects of CMI addition on $CaCO_3$ induction times.

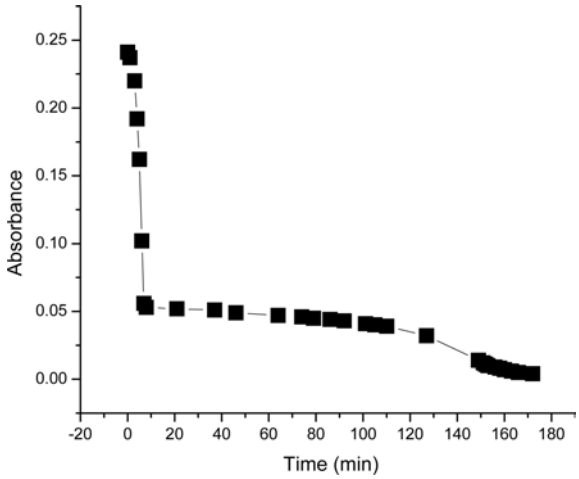

Fig. 17. Effect of the CMI biopolymer on the dissolution of deposited $CaCO_3$.

monitored as a function of time. Fig. 17 shows that a dramatic scale cleaning effect took place very rapidly (within 6 min), followed by a slower cleaning process (~160 min). The rapid process is assigned to removal of $CaCO_3$ layers that were deposited at the later stages of the deposition process, and therefore present the more "freshly" deposited $CaCO_3$. On the other hand, the slower process may correspond to removal of $CaCO_3$ layers that were deposited at the early stages of deposition, having sufficient time to mature and harden.

These results show the potential of CMI as a "green" $CaCO_3$ scale dissolver.

4. Conclusions/perspectives

The present paper is part of our continuing research efforts to identify and exploit novel chemistries as effective mineral scale growth inhibitors in process waters [11–13]. Herein, the emphasis is given on inhibitors that have no, or mild, environmental impact.

Formation of colloidal SiO_2 is a result of several complicated equilibria that are very sensitive to pH and tend to be accelerated by metal ions that form hydroxides, e.g., Fe^{2+}, Mg^{2+} or Al^{3+} [36–40]. The starting point is silicic acid self-condensation and is catalyzed by OH^- in the pH range of 5–10. Silica scale formation involves condensation between Si–OH groups formed at the material surface and Si–OH of the dissolved silicate present in water.

PAMAM-1 and 2 dendrimers combined with anionic polymers, such as CMI, seem to have a significant inhibitory effect on SiO_2 formation, most likely at its earlier stages where the reaction products are oligomeric silicates.

CMI assists the action of PAMAM-1 and 2 by alleviating formation of insoluble SiO_2–PAMAM precipitates. This most likely occurs by partial neutralization of the positive charge that exists in $-NH_3^+$ surface groups. However, if CMI dosage exceeds 40 ppm, the activity of PAMAM-1 drops dramatically. In that case CMIs negative charge "overwhelms" the dendrimer and poisons its inhibition ability. The activity of the PAMAM-2 dendimer does not seem to be as sensitive to CMI "overdosing".

Colloidal SiO_2 dissolution is a difficult task when applied to deposits in process water systems. Alternative chemistries sought herein involve polycarboxylates and carboxylate/phosphonate hybrids. These show variable activities, with 2-phosphonobutane-1,2,4-tricarboxylic acid being the most effective dissolver. Colloidal SiO_2 dissolution is catalyzed by hydroxyl ions, as shown in Fig. 18.

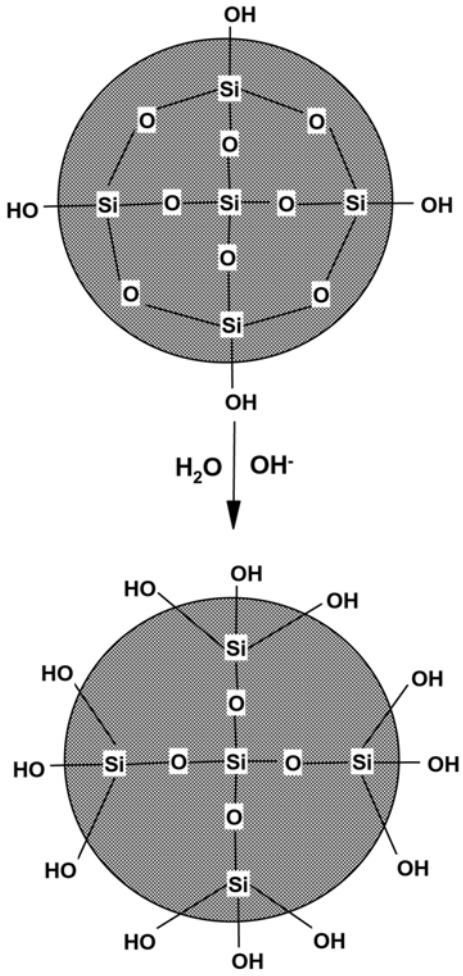

Fig. 18. Schematic representation of dissolution of a colloidal SiO_2 particle. This scheme represents the surface hydrolysis of Si-O-Si groups augmented by OH^- ions. Eventually, soluble $[SiO_4H_x]^{-(4-x)}$ are generated.

$$Si-O-Si + H_2O \xrightarrow{OH^-} 2\,Si-OH$$

However, their function is assisted by the presence of additives in a fashion that is not entirely clear. The details of such a dissolution mechanism are currently under investigation in our laboratory.

Acknowledgments

The Department of Chemistry, University of Crete, for financial support, and Dr. Mike Postingl of Custom Sensors & Technology for supplying the scale sensor.

References

[1] J.C. Cowan and D.J. Weintritt, Water-Formed Scale Deposits, Gulf Publishing, Houston, TX, 1976.
[2] Z. Amjad, ed., Mineral Scale Formation and Inhibition, Plenum Press, New York, 1995 [and references therein].
[3] R.Y. Ning, Desalination, 151 (2002) 67.
[4] R.Y. Ning and P.T.L. Shen, Ultrapure Water, 15(4) (1998) 37.
[5] W.S. Midkiff and H.P. Foyt, Mat. Perf., August (1979) 39.
[6] Z. Amjad, ed., Advances in Crystal Growth Inhibition Technologies, Plenum Press, New York, 2000 [and references therein].
[7] M.A. Quraishi, I.H. Farooqi and P.A. Saini, Corrosion, 55 (1999) 493.
[8] K.D. Demadis, Chemical Process., May (2003) 29.
[9] K.D. Demadis, Mat. Perf., April (2004) 38.
[10] K.D. Demadis and E. Neofotistou, Coll. Surf. A: Physiochem. Eng. Asp., 242 (2004) 213.
[11] K.D. Demadis, in: Compact Heat Exchangers and Enhancement Technology for the Process Industries, R.K. Shah, ed., Begell House, 2003, p. 483.
[12] K.D. Demadis and S.D. Katarachia, Phosphorus, Sulfur, Silicon, 179 (2004) 627.
[13] E. Neofotistou and K.D. Demadis, Desalination, 167 (2004) 257.
[14] W. Frenier, Technology for Chemical Cleaning of Industrial Equipment, NACE, Houston, 2000.
[15] C. Wohlberg and J.R. Buchholz, Corrosion/75, Paper No. 143, National Association of Corrosion Engineers, Houston, TX, 1975.
[16] C.W. Smith, Ind. Water Treatmet, July/August (1993) 20.
[17] W.S. Midkiff and H.P. Foyt, Mat. Perf., August (1979) 39.
[18] O.A. Matthews, A.N. Shipway and J.F. Stoddard, Prog. Polym. Sci., 23 (1998) 1.
[19] http://www./polychemistry.com/aquazol5-50.htm.
[20] F.R. Johannsen, Food Chem. Toxicol., 41 (2003) 49.
[21] H. El Shall, M.M. Rashad and E.A. Abdel-Aal, Cryst. Res. Technol., 37 (2002) 1264.
[22] L. Huber, Tenside Detergents, 12 (1975) 316.
[23] J. Steber and P. Wierich, Chemosphere, 15 (1986) 929.
[24] J. Steber and P. Wierich, Chemosphere, 16 (1987) 1323.
[25] K.D. Demadis and P. Lykoudis, Bioinorg. Chem. Appl., in press.
[26] M. Brooke, Corrosion/84, Paper No. 327, National Association of Corrosion Engineers, Houston, TX, 1984.
[27] P.R. Young, Corrosion/93, Paper No. 466, National Association of Corrosion Engineers, Houston, TX, 1993.
[28] P.R. Young, C.M. Stuart, P.M. Eastin and M. McCormick, Cooling Technology Institute Annual Meeting, Technical Paper, TP93-11, 1993.
[29] R. Sheikholeslami and S. Tan, Desalination, 126 (1999) 267.
[30] H. Kristmanndóttir, M. Ólafsson and S. Thórhallsson, Geothermics, 18 (1989) 191.
[31] H. Kristmanndóttir, Proc. 3rd Int. Symp. Water–Rock Interactions, 1980, p. 110.
[32] R.K. Iler, The Chemistry of Silica (Solubility, Polymerization, Colloid and Surface Properties and Biochemistry), Wiley–Interscience, New York, 1979.
[33] R.K. Iler, The Chemistry of Silica and Silicates, Cornell University Press, 1955.
[34] US Patents, Nos.: 4,983,646; 4,795,789; 4,756,881; 4,490,308.
[35] L. Dubin, Corrosion/80, Paper No. 222, National Association of Corrosion Engineers, Houston, TX, 1980.
[36] H.E. Bergna, in: The Colloid Chemistry of Silica, H.E. Bergna, ed., ASC, Washington, DC, 1994, p. 1.
[37] S.H. Chan, Z.J. Chen and P. He, J. Heat Transfer, 117 (1995) 323.
[38] D.L. Gallup, Geothermics, 27 (1998) 485.
[39] D.L. Gallup, Geothermics, 26 (1997) 483.
[40] R. Sheikholeslami, I.S. Al-Mutaz, S. Tan and S.D. Tan, Desalination, 150 (2002) 85.